Possible trajectories for Electric Solar Wind Sail validation

Lorenzo Niccolai[(1)*], Alessandro A. Quarta[(1)], Giovanni Mengali[(1)], Francesco Petrucciani[(2)]

[(1)] *Department of Civil and Industrial Engineering, University of Pisa, I-56122 Pisa, Italy*

[(2)] *European Space Operation Centre (ESOC), D-64293 Darmstadt, Germany*

Abstract

The aim of this paper is the analysis of a potential mission scenario that could be used to perform an in-situ test of the Electric Solar Wind Sail. Such an advanced propulsive system works only outside the Earth's magnetosphere, so a translunar mission (where the spacecraft is supposed to be inserted as a secondary "piggyback" payload) is hypothesized, in which at least a part of the spacecraft trajectory is around or beyond the Moon's orbit. The analysis of possible selenocentric trajectories is conducted with a three-dimensional generalization of the classical patched conic approximation. In particular, two cases are considered: a closed selenocentric orbit, and a Moon flyby that inserts the spacecraft on a post-flyby geocentric orbit with at least some branches outside the Earth's magnetosphere.

Keywords: Electric solar wind sail, Translunar trajectories, Mission analysis

1. Introduction

The Electric Solar Wind Sail (E-sail) is an innovative propulsion system concept, originally proposed by Pekka Janhunen in 2004 [1], see Fig. 1. This thruster exploits the interaction between the solar wind ions and a number of positively charged tethers to generate a propulsive acceleration without any propellant consumption, see Fig. 2(a). As a propellantless propulsion system, the E-sail concept is a good candidate for envisaging new mission scenarios that could be difficult or even impossible to achieve with more conventional (either chemical or electric) propulsion systems, including non-Keplerian orbits [2, 3], outer Solar System exploration [4, 5], planetary [6] or cometary [7] rendezvous, and even some exotic hypothetical applications in an interstellar travel [8]. The propulsive acceleration generated by an E-sail is a function of the inverse Sun-spacecraft distance, the sail design parameters and its attitude [9], under the hypothesis of perfectly flat sail. However, even if the latter assumption is removed, the effects on the tether inflection on the generated thrust is negligible [10, 11].

A first validation test of the E-sail working principle was tried in 2013 with the ESTCube-1 satellite [12], but a failure occurred, probably due to vibrational loads during the launch phase. The lack of experimental data should hopefully be overcome by the Finnish Aalto-1 satellite [13, 14]. Note that the E-sail technological tests so far conceived involve a single charged tether that interacts with the ionized atmosphere to obtain a small braking force on the spacecraft, the so called "plasma brake effect" [15], see Fig. 2(b), which could be useful for spacecraft deorbiting from low Earth orbits [16, 17, 18].

A problem that could arise during in-situ measurements lies in the use of a low-Earth orbit for the experimental test, as it happens for the Aalto-1 satellite, since in that case the flux of ions is significantly shielded by the Earth's magnetic field. For these reasons the aim of this paper is to define a mission scenario in which the spacecraft moves outside the Earth's magnetosphere for a time interval sufficient to complete

*Corresponding author

Email addresses: lorenzo.niccolai@ing.unipi.it (Lorenzo Niccolai[(1)]), a.quarta@ing.unipi.it (Alessandro A. Quarta[(1)]), g.mengali@ing.unipi.it (Giovanni Mengali[(1)]), francesco.petrucciani@esa.int (Francesco Petrucciani[(2)])

Published in Aerotecnica Missili & Spazio, Vol. 98, No. 2 June 2019, pp. 139–145. doi: https://doi.org/10.1007/s42496-019-00012-7

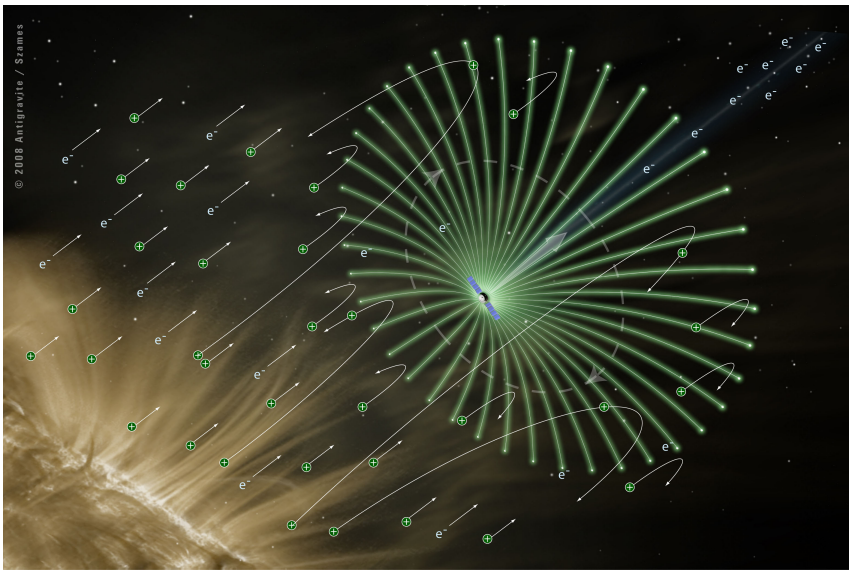

Figure 1: Artistic rendering of an Electric Solar Wind Sail. Courtesy of Alexandre Szames, Antigravité (Paris).

some significant in-situ measurements of the propulsive acceleration, using the actual solar wind flux. In this context, the possibility of obtaining an effective and low-cost test mission of an E-sail could raise the interest of space community on this innovative propulsion system. A possible target for such a testing mission is the Moon, which can be exploited with a gravity assist, after which the spacecraft reaches the boundary of the Earth's magnetosphere. This mission target could be also achieved with a closed selenocentric orbit, since the Moon is largely outside the Earth's magnetosphere when it is between the Earth and the Sun [19]. In both cases the spacecraft eventually covers a trajectory with some arcs being outside the Earth's magnetosphere.

The analysis of a translunar trajectory is one of the most studied subjects in spaceflight mechanics. In a preliminary analysis, the problem is addressed with a planar approach [20], using the concept of sphere of influence and a patched conic method in which the Earth-Moon transfer is assumed to be a Keplerian geocentric trajectory until the spacecraft enters into the Moon's sphere of influence. In particular, this work generalizes the classical patched conic method by accounting for the 3D nature of the problem. The obtained results are still in an analytical (and approximate) form, but are more accurate than those reported in Ref. [20] in terms of selenocentric and post-flyby trajectory determination, especially when the transfer trajectory and the Moon's geocentric orbit have different inclinations. The closed form solution of the results is useful for investigating a number of different mission scenarios with a substantial reduction of computational time with respect to a numerical integration of the equations of motion. In particular, such a simple analytical method to analyze translunar trajectories could constitute a useful tool for planning an E-sail in-situ test. In fact, although the simulations need a modest computational time, they are accurate enough for a preliminary mission design phase. As a result, the most promising trajectories can easily be identified and prepared for an in-depth analysis, which usually requires more complex and computationally-expensive tools.

The proposed mission strategy consists of exploiting a primary lunar mission to minimize the launch costs by inserting a piggyback spacecraft into a classical translunar trajectory. In this context, the preliminary analysis of potential mission scenarios is based on available data of future planned lunar missions. The possible selenocentric trajectories, which differ in launch date, initial conditions, and geometric conditions at the entrance in the Moon's sphere of influence, are analyzed with the 3D patched conic approximation, in order to identify the most promising ones. The proposed approach is tested with a hypothetical mission scenario in which the spacecraft is the secondary load of the Chinese lunar mission Chang'e-5 [21], whose launch was initially scheduled for November 2017 (and the simulations refer to this date). Although the launch date of Chang'e 5 has been delayed, the main objective of the numerical simulations is to prove the effectiveness of the proposed algorithm in finding the more promising translunar trajectories, which require

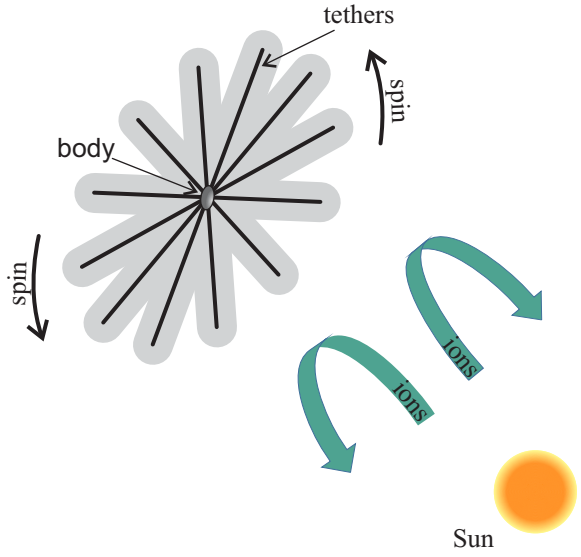

(a) E-sail.

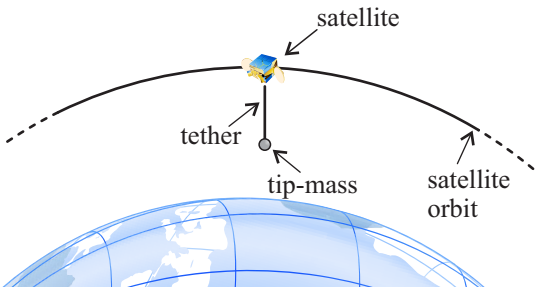

(b) Plasma Brake.

Figure 2: Conceptual sketch of an Electric Solar Wind Sail and Plasma Brake.

more complex simulations in the succeeding phases of the mission design. The results presented in this paper show both the feasibility of an E-sail testing translunar mission, and the good performance of the 3D approximate method in a preliminary mission design phase, where a number of different trajectories are considered.

2. Translunar missions: 3D mathematical model

Consider a launch vehicle covering a geocentric circular parking orbit with radius r_0 at time t_0, see Fig. 3. After a certain (given) coasting angle ψ_c is swept, an impulsive maneuver inserts the payload (spacecraft) into a coplanar translunar orbit with an initial velocity v_0 and a flight path angle ϕ_0.

The classical approach for the analysis of a translunar trajectory discussed in Ref. [20], based on the patched conic method and the sphere of influence approximation, is purely two-dimensional. In particular, the Earth-Moon transfer is assumed to be dominated by the Earth's gravity until the intercept (the point where the spacecraft enters into the Moon's sphere of influence). The 2D method is based on the fundamental assumption that the spacecraft transfer orbit, the Moon's geocentric orbit, and (consequently) the spacecraft selenocentric trajectory all lie on the same plane. Since the inclination of the Moon's orbit varies between 18.2 deg and 28.5 deg, the transfer orbit inclination must be comprised in this range if the classical approach is used. Clearly, this is a rough assumption, since possibly the intercept conditions of the mission scenario require a significantly different orbital inclination of the transfer trajectory.

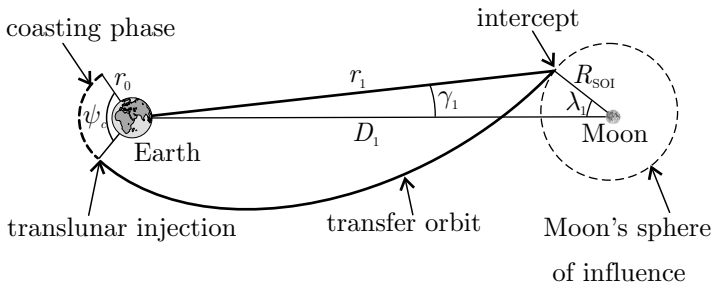

Figure 3: Translunar trajectory sketch, adapted from Ref. [20].

Given all the previous considerations, the introduction of an analytical approximated method that accounts for the 3D nature of the problem could provide an important tool for preliminary translunar trajectory analysis. The approach used in this work is based on less restrictive hypotheses compared to those introduced in Ref. [20], that is, the Moon's center of mass at intercept lies on the transfer orbit plane, and the transfer orbit is still coplanar with the parking orbit (it is assumed that the engines of the launch vehicle are capable of providing any required plane change before the insertion on the parking orbit). Under these assumptions, the analysis of the geocentric phase is analogous to the one made with a 2D approach. The radius of the Moon's sphere of influence is determined with the well-known formula $R_{\text{SOI}} \simeq D_1 \, (\mu_{\leftmoon} / \mu_{\oplus})^{0.4}$, where D_1 is the Earth-Moon distance (given by lunar ephemeris) at the intercept time t_1, $\mu_{\leftmoon}$ (or $\mu_{\oplus}$) is the Moon (or Earth) gravitational parameter. Taking into account that the semimajor axis a_T and eccentricity e_T of the spacecraft transfer orbit (subscript T) are [20]

$$a_T = \frac{\mu_{\oplus} \, r_0}{2 \, \mu_{\oplus} - r_0 \, v_0^2} \tag{1}$$

$$e_T = \sqrt{1 + \frac{r_0^2 \, v_0^2 \, \cos^2 \phi_0}{\mu_{\oplus} \, a_T}} \tag{2}$$

the conditions, in terms of Earth-spacecraft distance (r_1) and velocity (v_1) at intercept point (subscript 1) are

$$r_1 = \sqrt{R_{\text{SOI}}^2 + D_1^2 - 2 \, R_{\text{SOI}} \, D_1 \, \cos \lambda_1} \tag{3}$$

$$v_1 = \sqrt{\frac{\mu_{\oplus}}{r_1} \left(2 - \frac{r_1}{a_T} \right)} \tag{4}$$

$$\phi_1 = \arccos \left(\frac{r_0 \, v_0 \, \cos \phi_0}{r_1 \, v_1} \right) \tag{5}$$

$$\gamma_1 = \arcsin \left(\frac{R_{\text{SOI}}}{r_1} \, \sin \lambda_1 \right) \tag{6}$$

where the angles $\{\phi_1, \gamma_1, \lambda_1\}$ are defined in Fig. 3. Note that retrograde transfer orbits (and trajectories where the intercept is in the descending phase) are neglected in this analysis, in order to reduce the propellant cost and the transfer time. Hence, the extraction of the inverse cosine in Eq. (5) is straightforward.

The transfer time Δt_T can be calculated as

$$\Delta t_T = \sqrt{\frac{a_T^3}{\mu_{\oplus}}} \, (E_1 - e_T \, \sin E_1 - E_0 + e_T \, \sin E_0) \tag{7}$$

where E is the eccentric anomaly, which is written as a function of the true anomaly ν as

$$\nu_{\{0,1\}} = \arccos\left[\frac{a_T\,(1-e_T^2)}{e_T\,r_{\{0,1\}}} - \frac{1}{e_T}\right] \tag{8}$$

$$E_{\{0,1\}} = 2\arctan\left(\sqrt{\frac{1-e_T}{1+e_T}}\,\tan\frac{\nu_{\{0,1\}}}{2}\right) \tag{9}$$

Since the parking orbit is circular, the flight time Δt_c of the coasting phase is

$$\Delta t_c = \sqrt{\frac{r_0^3}{\mu_\oplus}}\,\psi_c \tag{10}$$

Finally, neglecting the time between launch and parking orbit insertion, the total transfer time Δt (and so the launch date t_0) can be calculated as

$$\Delta t = \Delta t_c + \Delta t_T \qquad , \qquad t_0 = t_1 - \Delta t \tag{11}$$

2.1. Intercept analysis

The velocity of the spacecraft with respect to the Moon is calculated as a vectorial difference between the geocentric velocity $\boldsymbol{v}_1$ and the Moon's orbital velocity $\boldsymbol{v}_{\leftmoon}$ at intercept (the latter is evaluated through an ephemeris calculation):

$$\boldsymbol{v}_2 = \boldsymbol{v}_1 - \boldsymbol{v}_{\leftmoon} \tag{12}$$

where the subscript 2 identifies the selenocentric quantity. Equation (12) can be more easily applied if a suitable reference frame $\mathcal{T}_{\leftmoon}\,(M; x, y, z)$ is introduced: the origin M coincides with the position of the Moon's center of mass at intercept, the y-axis is parallel to the vector $\boldsymbol{v}_{\leftmoon}$, the z-axis is orthogonal to the Moon's orbital plane, and the x-axis completes the right-handed reference frame. The components of the vector $\boldsymbol{v}_1$ in such a reference frame depend of the angle $\theta \in [-\pi, \pi]$ formed by the transfer orbit plane and the Moon's geocentric orbit plane, which can be evaluated as the difference between the spacecraft azimuth β_1 and the Moon's azimuth $\beta_{\leftmoon}$ at intercept, see Fig. 4.

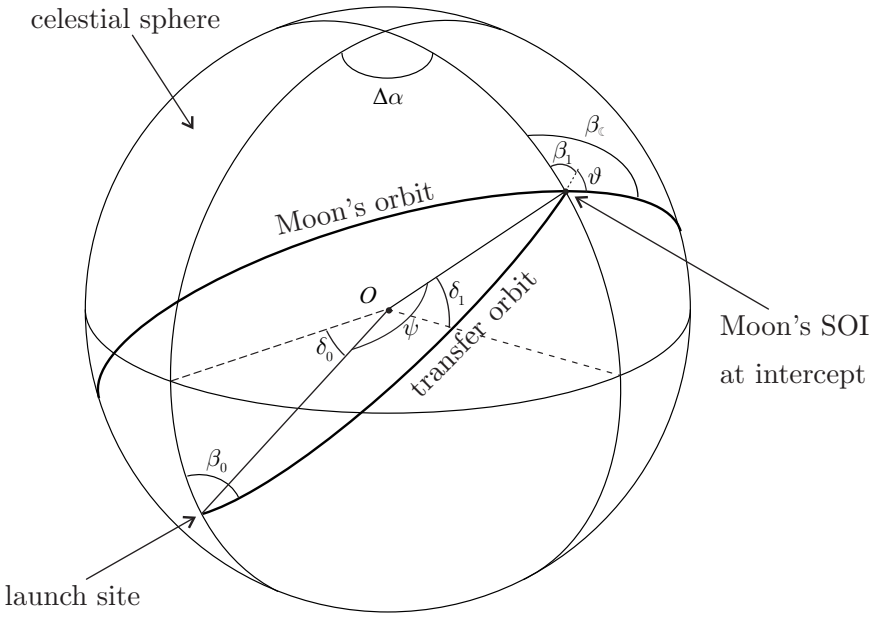

Figure 4: Sketch of the geometric quantities involved in the intercept parameters determination.

Note that the azimuth β is the angle between the local meridian on the celestial sphere and the velocity of the object [20]. Using spherical geometry considerations, the angles $\{\beta_1, \beta_{\leftmoon}, \theta\}$ are calculated as functions of ψ

$$\psi = \psi_c + \nu_1 - \nu_0 \tag{13}$$

$$\beta_1 = \arccos\left(\frac{\sin\delta_1\,\cos\psi - \sin\delta_0}{\cos\delta_1\,\sin\psi}\right) \tag{14}$$

$$\beta_{\leftmoon} = \arctan\left(\frac{\sin\Delta\alpha_{\leftmoon}}{\sin\delta_1\cos\Delta\alpha_{\leftmoon} - \cos\delta_1\,\tan\delta_{0\leftmoon}}\right) \tag{15}$$

$$\theta = \beta_{\leftmoon} - \beta_1 \tag{16}$$

where $\Delta\alpha_{\leftmoon}$ is the difference in Moon's right ascension between the intercept and the launch date, $\delta_{0\leftmoon}$ is the Moon's declination at launch, and δ_1 is the Moon's declination at intercept evaluated through an ephemeris calculation.

When θ is known, the vectorial difference of Eq. (12) can be determined if a suitable assumption is introduced, that is, being the Moon's orbital eccentricity very small [20], the Moon's geocentric velocity is nearly orthogonal to the Earth-Moon vector, which implies that the x-axis of the reference frame $\mathcal{T}_{\leftmoon}(M; x, y, z)$ coincides with the Earth-Moon direction, pointing towards the Moon. Therefore, the vectors involved in Eq. (12) are written in $\mathcal{T}_{\leftmoon}(M; x, y, z)$ as

$$\boldsymbol{v}_1 = \begin{bmatrix} v_1\,\sin(\phi_1-\gamma_1) \\ v_1\,\cos(\phi_1-\gamma_1)\,\cos\theta \\ v_1\,\cos(\phi_1-\gamma_1)\,\sin\theta \end{bmatrix} \qquad \boldsymbol{v}_{\leftmoon} = \begin{bmatrix} 0 \\ v_{\leftmoon} \\ 0 \end{bmatrix} \qquad \boldsymbol{v}_2 = \begin{bmatrix} v_1\,\sin(\phi_1-\gamma_1) \\ v_1\,\cos(\phi_1-\gamma_1)\,\cos\theta - v_{\leftmoon} \\ v_1\,\cos(\phi_1-\gamma_1)\,\sin\theta \end{bmatrix} \tag{17}$$

With similar geometric considerations, the spacecraft position vector $\boldsymbol{r}_2$ at intercept has the following components in $\mathcal{T}_{\leftmoon}(M; x, y, z)$

$$\boldsymbol{r}_2 = \begin{bmatrix} -R_{\text{SOI}}\,\cos\lambda_1 \\ R_{\text{SOI}}\,\sin\lambda_1\,\cos\theta \\ R_{\text{SOI}}\,\sin\lambda_1\,\sin\theta \end{bmatrix} \tag{18}$$

The vectors $\boldsymbol{r}_2$ and $\boldsymbol{v}_2$ define the orbital plane of the Keplerian selenocentric trajectory (subscript M), whose semimajor axis a_M and eccentricity e_M are obtained as [20]

$$a_M = \frac{\mu_{\leftmoon}\,r_2}{2\,\mu_{\leftmoon} - r_2\,v_2^2} \tag{19}$$

$$e_M = \sqrt{1 + \frac{r_2^2\,v_2^2\,\sin\epsilon_2}{\mu_{\leftmoon}\,a_M}} \tag{20}$$

where ϵ_2 is the angle between $\boldsymbol{r}_2$ and $\boldsymbol{v}_2$ given by

$$\epsilon_2 = \frac{\arccos(\boldsymbol{r}_2 \cdot \boldsymbol{v}_2)}{\|\boldsymbol{r}_2\|\,\|\boldsymbol{v}_2\|} \tag{21}$$

Note that the angle ϵ_2 is conceptually analogue to the one presented in Ref. [20], but it accounts for a 3D spacecraft-Moon encounter. The calculation of the periselenium radius r_p and velocity v_p is straightforward

$$r_p = a_M\,(1 - e_M) \qquad , \qquad v_p = \sqrt{\frac{\mu_{\leftmoon}}{r_p}\,\left(2 - \frac{r_p}{a_M}\right)} \tag{22}$$

Alternatively, one could focus on the post-flyby characteristic quantities, that is, the hyperbolic excess velocity v_∞ and the turn angle χ

$$v_\infty = \sqrt{\frac{\mu_{\leftmoon}}{R_{\text{SOI}}}\,\left(2 - \frac{R_{\text{SOI}}}{a_M}\right)} \qquad , \qquad \chi = 2\,\arcsin\left(\frac{1}{e_M}\right) \tag{23}$$

2.2. Feasible trajectory selection

The feasible translunar trajectories can be selected following a procedure that is conceptually similar to the one presented in Ref. [20]. First, the launch site must be fixed, in terms of latitude δ_0 and longitude λ_0. Usually, every launch site has specific safety limitations concerning the allowable launch azimuth β_0 that can be expressed by imposing a minimum value $\beta_{\min}$ and a maximum value $\beta_{\max}$. Hence, if the selected mission scenario requires a launch azimuth $\beta_0 \in [\beta_{\min}, \beta_{\max}]$, the translunar trajectory meets the safety rules of the chosen launch site. In order to determine β_0, one should calculate the total angle ψ swept during the transfer phase

$$\psi = \psi_c + \nu_1 - \nu_0 \tag{24}$$

where ν_0 and ν_1 are given by Eq. (8). The flight azimuth at launch can be expressed as [20]

$$\beta_0 = \arccos\left(\frac{\sin\delta_1 - \sin\delta_0\,\cos\psi}{\cos\delta_0\,\sin\psi}\right) \tag{25}$$

where δ_1 is the declination of both the spacecraft and the Moon at intercept time t_1, see Fig. 4.

When the intercept time t_1 is known, it is possible to evaluate the difference $\Delta\alpha$ in right ascension between the intercept and the launch site (see Fig. 4), using the basic concepts of spherical geometry in analogy with Ref. [20]

$$\Delta\alpha = \arccos\left(\frac{\cos\psi - \sin\delta_0\,\sin\delta_1}{\cos\delta_0\,\cos\delta_1}\right) \tag{26}$$

The angle $\Delta\alpha$ can also be calculated as the difference between the Moon's right ascension at intercept α_1 and the launch site right ascension at launch

$$\Delta\alpha = \alpha_1 - \lambda_g - \lambda_0 \tag{27}$$

where λ_{g_0} is the launch site Greenwich Sidereal Time at launch and α_1 is given by lunar ephemeris. The selected mission scenario is feasible only if, comparing the two values of $\Delta\alpha$ given by Eqs. (26) and (27), the (absolute) difference is less than 1 deg [20]. If the difference is larger, some input parameters must be adjusted (for example, the coasting angle, the launch date, or the angle λ_1), in order to obtain a physically acceptable translunar trajectory.

3. Mission application

The 3D method presented in the previous Section is tested with a potential mission scenario in which a spacecraft equipped with an E-sail tether is a secondary payload (piggyback) of one of the launches of the planned Chinese lunar program. In particular, the starting date is selected in November 2017 [21], corresponding to the initially hypothesized launch window for the Chang'e-5 mission, later delayed at December 2019. The launch site is Wenchang, China, and the launch vehicle is a Long March CZ-5 launcher. The characteristics of the launch site and the initial conditions used for the simulations, mainly based on the available data about the launch site and launch vehicle, are listed in Table 1.

Launch site				Initial conditions			
δ_0 [deg]	λ_0 [deg]	$\beta_{\min}$ [deg]	$\beta_{\max}$ [deg]	r_0 [km]	ψ_c [deg]	v_0 [km/s]	ϕ_0 [deg]
19.6	111.0	0.0	180.0	6573.1	42.9	11.0	0.0

Table 1: Launch site data and initial conditions used for the translunar trajectories simulations.

The remaining two input parameters for the translunar trajectory simulations, that is, the intercept time t_1 and the angle λ_1, are varied in order to analyze a number of possible feasible trajectories. In particular, the value of λ_1 is varied for each intercept time from 0 to 90 deg with a step size of 5 deg. The intercept time is varied within the month of November 2017, with a time-step of 1 hour between two successive simulations. The feasible scenarios are simulated with an orbital propagator that numerically integrates the equations of motion. The most promising scenarios, in terms of small discrepancies between the numerical propagator

and the 3D method, are investigated in order to identify the best option for the E-sail testing mission. The waiting times required for exiting the Earth's magnetosphere are calculated using a simplified (analytical) magnetosphere model that consists of the superposition of a constant magnetic field and a dipole magnetic field [22], where the free parameters required to fully define the model are selected to make the magnitude of the interplanetary magnetic inductance vector in the vicinity of the Earth coincident with the mean value of 6 nT, in accordance with Ref. [23].

The first scenario involves a circularizing maneuver at the periselenium, that allows the spacecraft to remain around the Moon, allowing a time out of the magnetosphere of about 15 days, largely sufficient to perform the tether experiment and to communicate the results to the ground station. Clearly, the Earth-spacecraft distance does not grow excessively, so that the communications with the ground station does not require a large antenna. However, an engine is required for the circularizing impulse. The chosen scenario involves a launch from Wenchang on 1 November 2017 at 11:42, and an intercept with $\lambda_1 = 30\,\text{deg}$, on 3 November 2017 at 3:00. The characteristics of the selected selenocentric orbit, calculated with the classical 2D approach, the 3D method presented in the previous Section, and the orbital propagator, are listed in Table 2.

	$r_p\,[\text{km}]$	$v_p\,[\text{km/s}]$	$\Delta v\,[\text{km/s}]$
2D	3462	2.29	1.11
3D	33895	1.65	1.27
num.	26662	1.87	1.44

Table 2: Periselenium conditions and circularizing Δv for the selected closed selenocentric scenario, evaluated with the 2D method, the 3D method, and the orbital propagator.

The second possibility consists in exploiting the Moon's mass with a gravity assist maneuver that inserts the spacecraft on a geocentric hyperbolic trajectory capable of quickly going out of the magnetosphere. Such an approach does not involve any propellant consumption, but the geocentric distance soon becomes large, so that the experiment must be performed within a few days, otherwise the communications of the data would be impossible. The selected orbit starts from Wenchang on 27 November 2017 at 9:30, and it arrives at intercept on 29 November 2017 at 4:00 with an angle $\lambda_1 = 40\,\text{deg}$. Table 3 summarizes the characteristics of the selected mission scenario. Note that, in this approximate simulation, the spacecraft exits the magnetosphere within 10 hours from the launch (before the lunar intercept), and so the experiment could realistically be performed on the translunar trajectory, or during the Moon's flyby, when the Earth-spacecraft distance is not too large.

	$v_\infty\,[\text{km/s}]$	$\chi\,[\text{deg}]$	$t_w\,[\text{hrs}]$
2D	1.54	13.9	NA
3D	1.54	9.3	NA
num.	1.81	7.0	10.0

Table 3: Flyby parameters and time required to exit the magnetosphere for the selected open selenocentric scenario, evaluated with the 2D method, the 3D method, and the orbital propagator.

According to the presented results, the open selenocentric orbit scenario seems the most promising one, because an onboard engine is not required for the spacecraft and the waiting time for the experiment is small. A sketch of the 3D trajectory for this mission scenario is presented in Fig. 5.

4. Conclusions

A generalization of the patched conic method for the analysis of a translunar trajectory is presented. Such an analytical approach uses the classical sphere of influence concept, but it accounts for a three-dimensional spacecraft-Moon encounter, and is capable of predicting the selenocentric orbit parameters with a higher accuracy with respect to a two-dimensional method.

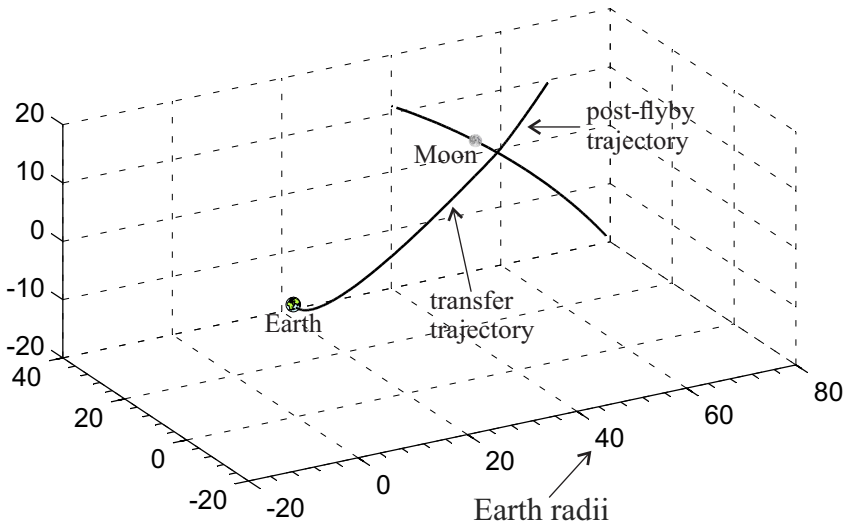

Figure 5: 3D sketch of the transfer and post-flyby trajectories for the selected scenario.

The 3D patched conic approach is used to analyze the possible translunar trajectories of an Electric Sail, an innovative propellantless propulsive system that requires a plasma stream (i.e. the solar wind) to produce thrust. In particular, the method is useful for testing the Electric Sail outside the Earth's magnetosphere. The spacecraft equipped with an E-sail tether should possibly be inserted as a secondary payload of a primary lunar mission, in order to minimize the launch costs. The simulations performed in the current work are based on the Chinese lunar mission Chang'e-5, whose launch was initially planned for November 2017. The preliminary results suggest the feasibility of such a mission scenario, presenting two possible alternatives: a closed selenocentric orbit obtained with a circularizing impulse, and a lunar flyby that eventually allows the spacecraft to reach the boundary of the Earth's magnetosphere. The preliminary results suggest that the latter could be the best option for the chosen mission scenario.

References

[1] P. Janhunen, Electric sail for spacecraft propulsion, Journal of Propulsion and Power 20 (4) (2004) 763–764, doi: 10.2514/1.8580.

[2] L. Niccolai, A. A. Quarta, G. Mengali, Electric sail-based displaced orbits with refined thrust model, Proceedings of the Institution of Mechanical Engineers, Part G: Journal of Aerospace Engineering 232 (3) (2018) 423–432, doi: 10.1177/0954410016679195.

[3] L. Niccolai, A. A. Quarta, G. Mengali, Electric sail elliptic displaced orbits with advanced thrust model, Acta Astronautica 138 (2016) 503–511, doi: 10.1016/j.actaastro.2016.10.036.

[4] A. A. Quarta, G. Mengali, Electric sail mission analysis for outer solar system exploration, Journal of Guidance, Control, and Dynamics 33 (3) (2010) 740–755, doi: 10.2514/1.47006.

[5] M. Bassetto, A. A. Quarta, G. Mengali, Locally-optimal electric sail transfer, Proceedings of the Institution of Mechanical Engineers, Part G: Journal of Aerospace Engineering 233 (1) (2017) 166–179, doi: 10.1177/0954410017728975.

[6] M. Huo, G. Mengali, A. A. Quarta, Optimal planetary rendezvous with an electric sail, Aircraft Engineering and Aerospace Technology 88 (4) (2016) 512–522, doi: 10.1108/AEAT-01-2015-0012.

[7] A. A. Quarta, G. Mengali, P. Janhunen, Electric sail option for cometary rendezvous, Acta Astronautica 127 (2016) 684–692, doi: 10.1016/j.actaastro.2016.06.020.

[8] N. Perakis, A. M. Hein, Combining magnetic and electric sails for interstellar deceleration, Acta Astronautica 128 (2016) 13–20, doi: 10.1016/j.actaastro.2016.07.005.

[9] M. Huo, G. Mengali, A. A. Quarta, Electric sail thrust model from a geometrical perspective, Journal of Guidance, Control, and Dynamics 41 (3) (2018) 734–740, doi: 10.2514/1.G003169.

[10] M. Bassetto, G. Mengali, A. A. Quarta, Thrust and torque vector characteristics of axially-symmetric E-sail, Acta Astronautica 146 (2018) 134–143, doi: 10.1016/j.actaastro.2018.02.035.

[11] M. Bassetto, G. Mengali, A. A. Quarta, Stability and control of spinning E-sail in heliostationary orbit, Journal of Guidance, Control, and Dynamics 42 (2) (2018) 425–431, doi: 10.2514/1.G003788.

[12] A. Slavinskis, M. Pajusalu, H. Kuuste, et al., Estcube-1 in-orbit experience and lessons learned, IEEE Aerospace and Electronic Systems Magazine 30 (8) (2015) 12–22, doi: 10.1109/MAES.2015.150034.

[13] A. Kestila, T. Tikka, P. Peitso, et al., Aalto-1 nanosatellite - technical description and mission objectives, Geoscientific Instrumentation, Methods and Data Systems 2 (2013) 121–130, doi: 10.5194/gi-2-121-2013.
[14] O. Khurshid, T. Tikka, J. Praks, M. Hallikainen, Accomodating the plasma brake experiment on-board the aalto-1 satellite, Proceedings of the Estonian Academy of Sciences 63 (2S) (2014) 258–266, doi: 10.3176/proc.2014.2S.07.
[15] P. Janhunen, Electrostatic plasma brake for deorbiting a satellite, Journal of Propulsion and Power 26 (2) (2010) 370–372, doi: 10.2514/1.47537.
[16] L. Orsini, L. Niccolai, G. Mengali, A. A. Quarta, Plasma brake model for preliminary mission analysis, Acta Astronautica 144 (2018) 297–304, doi: 10.1016/j.actaastro.2017.12.048.
[17] L. Niccolai, M. Bassetto, A. A. Quarta, G. Mengali, Plasma brake approximate trajectory. part i: Geocentric motion, in: 4th IAA Conference on University Satellite Missions and CubeSat Workshop, no. 163, Rome, Italy, 2017, pp. 235–247.
[18] M. Bassetto, L. Niccolai, A. A. Quarta, G. Mengali, Plasma brake approximate trajectory. part ii: Relative motion, in: 4th IAA Conference on University Satellite Missions and CubeSat Workshop, Vol. 163, Rome, Italy, 2017, pp. 249–259.
[19] O. Schneider, Interaction of the moon with the earth's magnetosphere, Space Science Reviews 6 (5) (1967) 655–704, doi: 10.1007/BF00168794.
[20] R. R. Bate, D. D. Mueller, J. E. White, Fundamentals of Astrodynamics, Dover Publications, Inc., 1971, Ch. 7, pp. 321–355.
[21] F. Li, M. Ye, J. Yan, W. Hao, J. P. Barriot, A simulation of the four-way lunar lander-orbiter tracking mode for the chang'e-5 mission, Advances in Space Research 57 (11) (2015) 2376–2384, doi: 10.1016/j.asr.2016.03.007.
[22] G. A. Katsiaris, Z. M. Psillakis, An analytic model of the earth's magnetosphere, Astrophysics and Space Science 132 (1) (1987) 165–175, doi: 10.1007/BF00637791.
[23] M. Harris, R. Lyle, et al., Magnetic fields - earth and extraterrestrial, Tech. Rep. SP-8017, NASA (1967).